Optimization of cell receptor-specific targeting through multivalent decoration of polymeric nanoparticles

Suzanne M. D'Addio[1], Steven Baldassano[1], Lei Shi[1], Lila Cheung[1], Douglas H. Adamson[1], Matthew Bruzek[2], John E. Anthony[2], Debra L. Laskin[3], Patrick J. Sinko[3], Robert K. Prud'homme[1]*

[1]Chemical and Biological Engineering, Princeton University, Princeton, NJ 08544

[2]Department of Chemistry, University of Kentucky, Lexington, KY, 40506

[3]Ernest Mario School of Pharmacy, Rutgers University, Piscataway, NJ, 08854

* Author for Correspondence, Department of Chemical Engineering, Princeton University, Princeton, NJ 08544 USA Tel: (609) 258-4577 Fax: (609) 258-0211 prudhomm@princeton.edu

Supplemental Information

S.1. Synthesis of compounds 1-4.

*S.1.1. Synthesis of 2'-bromoethyl 2,3,4,6-tetra-O-acetyl-a-D-mannopyranoside **(1)*** [1].

First, 0.632 mL of 2-bromoethanol (95%, Sigma) was injected into a solution of 1,2,3,4,6-penta-*O*-acetyl-α/β-D-mannopyranoside (5.12 mmol, 99.9%, IRIS Biotech GmbH) in 25 mL of dry DCM. Boron trifluoride etherate (17.9 mmol, >99%, $BF_3 \cdot OEt_2$, Sigma) was added to the mixture under argon. The reaction mixture was stirred in the dark for 24 h. An additional 40 mL of DCM was added, and the reaction mixture was quenched by adding 40 mL saturated sodium bicarbonate. The organic phase was washed with DI water (2 × 50 mL), dried over $MgSO_4$, filtered and concentrated to dryness under reduced pressure. The resulting oil was then purified using column chromatography with a hexane/ethyl acetate (from 4:1 to 1:1, v/v) mobile phase and dried to obtain **1** as a white powder.

*S.1.2. Synthesis of 2'-azidoethyl 2,3,4,6-tetra-O-acetyl-a-D-mannopyranoside **(2)*** [1].

1 (1.7g) was dissolved in 50 mL of DMSO. Sodium azide (1.2 g, 99.5%, Sigma) was added under argon atmosphere. The reaction mixture was stirred in the dark at 60 °C for 4 h followed by room temperature for 24 h. Water (100 mL) was added and the product was extracted twice with DCM. The combined organic layer was washed with deionized water (4 × 100 mL), dried over $MgSO_4$, filtered and concentrated to dryness. (Yield: 89 %).

*S.1.3. Synthesis of 2'-azidoethyl a-D-mannopyranoside **(3)*** [2].

2 (1.0 g) was dissolved in 10 mL of dry methanol followed by the addition of 0.192 mL of sodium methoxide in methanol (5M, Aldrich) under Ar. The reaction continued at room temperature overnight. To neutralize, 15 mL of methanol and ~ 83 mg of Amberlite IR-120 H^+

was added (pH ≈ 7). The resin was filtered off and the solvent evaporated to afford the product quantitatively as a white solid (Yield: 90 %).

*S.1.4. Synthesis of $PS_{1.5k}$-b-PEG_{5k}-alkyne (**4**)* [3].

$PS_{1.5k}$-*b*-PEG_{5k}-**OH** (2 g) was dissolved in 50 mL of anhydrous THF. NaH in mineral oil (2.2 mmol, 60%, Sigma) was added to the solution, stirred in a 0 °C bath, and after 40 min propargyl bromide solution (222 μL, 80 wt%, Aldrich) was injected slowly to the mixture. The reaction continued at room temperature for 24 h and was quenched by addition of 10 mL of water. The solution was dried and the residue was extracted with DCM (80 mL × 2). The organic phase was washed wit0h 80 mL of H_2O, dried over Na_2SO_4 and concentrated. The product was precipitated in 150 mL of ether, concentrated by a centrifuge (twice) and vacuum dried give a white/yellow powder (Yield: 53 %).

S.2. Synthesis of Tris[(1-benzyl-1H-1,2,3-triazol-4-yl)methyl] amine (TBTA) [4].

Tripropargylamine (4.3g, 97%, Alfa Aesar) was added to 50 mL of Acetonitrile. Benzyl azide (18.8 mL, 94%, Alfa Aesar), 2,6 lutidine (3.8 mL, > 98%, Alfa Aesar) and $Cu(MeCN)_4PF_6$ (0.5g, 97%, Sigma) were added, and the hot reaction mixture was cooled in an ice bath and stirred at room temperature for 3 days. Volatile components of the mixture were removed by rotary evaporation. The residue was washed with acetonitrile, filtered and recrystallized from t-butyl alcohol/water (1:1, v/v) by the addition of water. A fine, off white powder was recovered (Yeild: 63%).

Scheme S.1. (a-b) Synthetic route for $PS_{1.5k}$-*b*-PEG_{5k}-**MAN** (a) Synthesis of 2'-azidoethyl α-D-mannopyranoside (**3**). (b) Conjugation to form $PS_{1.5k}$-*b*-PEG_{5k}-**MAN** (**5**) *via* the click reaction. (c) O-methylation reaction to produce PS_m-*b*-PEG_n-**OCH_3** (**6**)

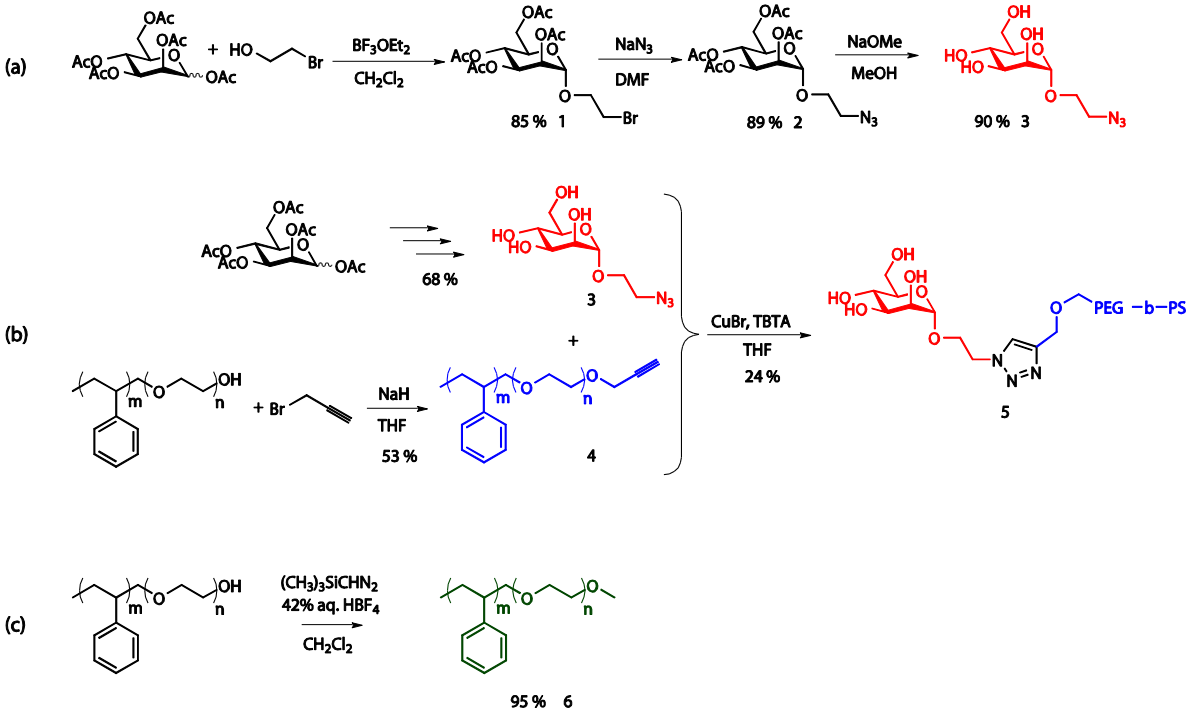

S.3. ^{1}H NMR Spectra

S.3.1. Characterization.

^{1}H NMR spectra were acquired on a Varian INOVA 500 MHz instrument.

*S.3.2. Synthesis of $PS_{1.5k}$-b-PEG_{5k}-**MAN***

The ^{1}H NMR spectra for products **1**, **2**, and **3** are plotted in Fig. S.1. All spectra were measured in CD_3OD. The peak assignments are as follows.

- *2'-bromoethyl 2,3,4,6-tetra-O-acetyl-α-D-mannopyranoside (**1**).* ^{1}H NMR (500 MHz, CD_3OD): δ 5.34 (dd, 1H), 5.28 (t, 3H), 5.26 (dd, 1H), 4.87 (d, 1H), 4.27 (dd, 1H), 4.15–4.11 (2H, m), 3.97 (ddd, 2H), 3.89 (ddd, 1H), 3.52 (t, 2H), 2.16 (s, 3H), 2.10 (s, 3H), 2.05 (s, 3H), 2.00 (s, 3H).
- *2'-azidoethyl 2,3,4,6-tetra-O-acetyl-a-D-mannopyranoside (**2**).* ^{1}H NMR (500 MHz, CD_3OD): δ 5.34 (dd, 1H), 5.29 (t, 1H), 5.26 (dd, 1H), 4.86 (d, 1H), 4.27 (dd, 1H), 4.11 (dd, 1H), 4.04 (ddd, 1H), 3.86 (ddd, 1H), 3.66 (ddd, 1H), 3.51-3.41 (m, 2H), 2.15 (s, 3H), 2.09 (s, 3H), 2.04 (s, 3H), 1.98 (s, 3H).
- *2'-azidoethyl a-D-mannopyranoside (**3**).* ^{1}H NMR (500 MHz, CD_3OD): δ 4.81 (d, 1H), 3.92 (ddd, 1H), 3.86-3.83 (m, 2H), 3.74-3.69 (m, 2H), 3.64-3.55 (m, 2H), 3.41 (t, 2H).

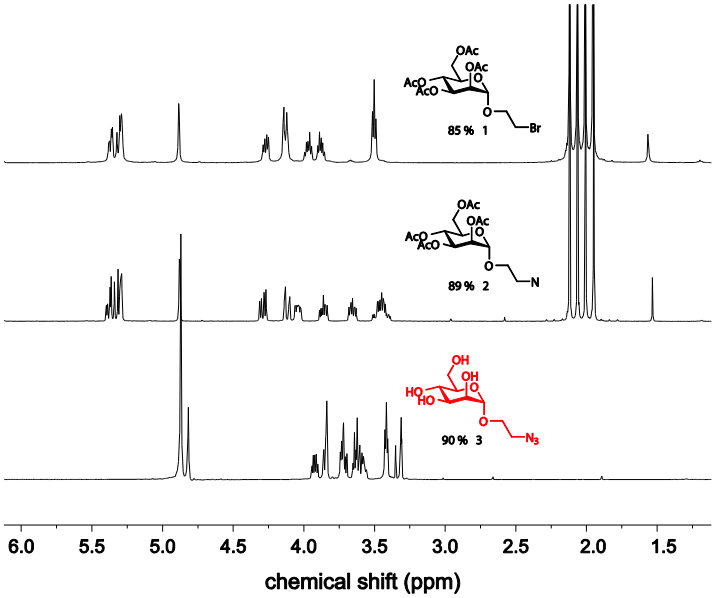

Figure S.1. ^{1}H NMR spectra for products **1**, **2**, and **3**.

The ^{1}H NMR spectra for TBTA, the catalyst for the click chemistry reaction, is plotted in Fig. S.2. The NMR spectrum was measured in $CDCl_3$ after recrystallization. The peak assignments are as follows.

- *Tris[(1-benzyl-1H- 1,2,3-triazol-4-yl)methyl] amine (TBTA*). ^{1}H NMR (500 MHz, $CDCl_3$): δ 7.66 (s, 3H), 7.53 (m, 9H), 7.27 (m, 11H, contains solvent peak), 5.51 (s, 6H), 3.70 (s, 6H).

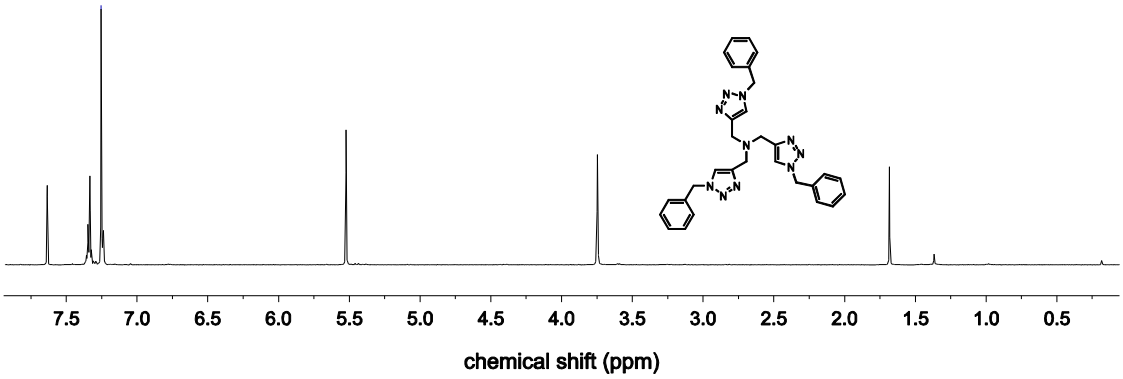

Figure S.2. The ^{1}H NMR spectra for TBTA.

The ^{1}H NMR spectra for the starting $PS_{1.5k}$-*b*-PEG_{5k}-**OH** polymer, product **4,** and the final product, **5** are plotted in Fig. S.3. The NMR spectra was measured in $CDCl_3$. The peak assignments are as follows.

- *$PS_{1.5K}$-b-PEG_{5K}-**OH***. ^{1}H NMR (500 MHz, $CDCl_3$): δ 7.25-6.25 (m, 72H), 3.65 (m, 302H), 2.27-0.57 (br, 57H, contains water).
- *$PS_{1.5K}$-b-PEG_{5K} -**alkyne (4)***. ^{1}H NMR (500 MHz, $CDCl_3$): δ 7.25-6.25 (m, 72H), 4.21 (d, 2H), 3.65 (m, 439H), 2.44 (s, 1H), 2.27-0.57 (br, 68H, contains water).
- *$PS_{1.5K}$-b-PEG_{5K} -**MAN (5)***. ^{1}H NMR (500 MHz, $CDCl_3$): δ 7.72 (s, 1H), 7.25-6.25 (m, 72H), 4.75 (s, 1H), 4.71 (d, 2H), 4.59 (m, 2H), 3.65 (m, 458H), 2.27-0.57 (br, 94H, contains water).

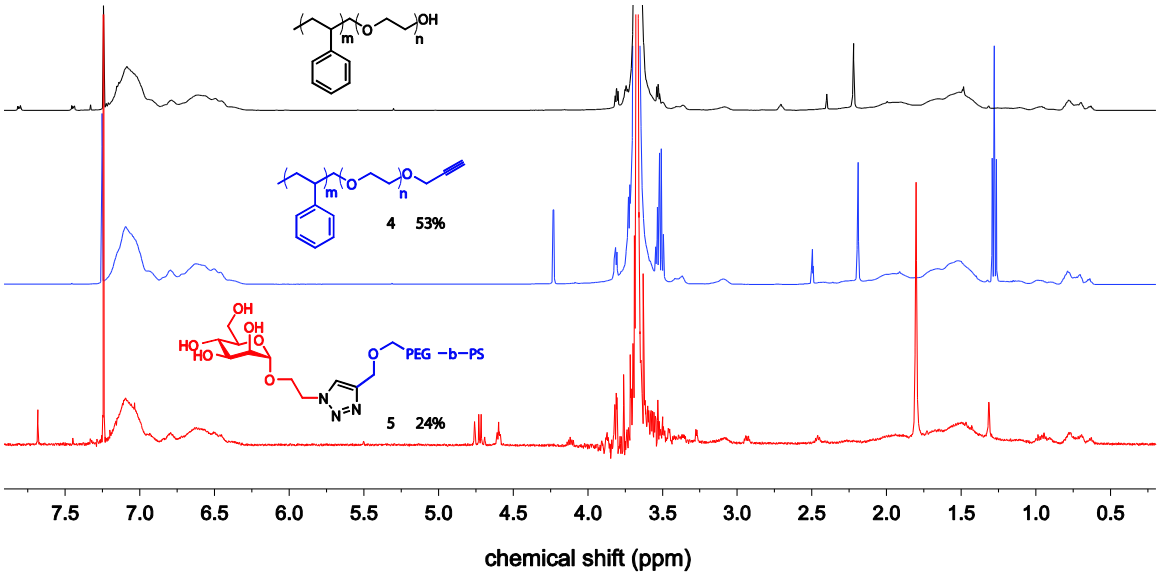

Figure S.3. The ^{1}H NMR spectra for $PS_{1.5k}$-b-PEG_{5k}-OH and compounds **4** and **5**.

*S.3.3. Synthesis of PS_m-b-PEG_n-**OCH_3***

Binding experiments at 4 °C with VE nanocarriers stabilized by $PLA_{3.8k}$-*b*-PEG_{5k}-**OCH_3** and $PS_{1.5k}$-*b*-PEG_{5k}-**OH** revealed that when the terminal group on PEG is **OCH_3**, there is not significant binding relative to when the terminal group on PEG is **OH** (Fig. . Given this finding, $PS_{1.5k}$-*b*-PEG_{5k}-**OCH_3** was synthesized as a "control" polymer for macrophage targeting experiments. These control groups were required for all non-functionalized surface polymers in order to isolate the effects of mannose ligand surface density on nanocarrier association with cells expressing the mannose receptor.

A protocol has been established by Aoyama and Shioiri [5] to be effective for the o-methylation of simple alcohols, but has not yet been evaluated for the modification of polymers. Therefore, the protocol was modified to enable high conversion of the hydroxyl end group on polymers. To determine the process conditions described for the reaction in Chapter 3.1, the conversion of the hydroxyl terminus on monomethoxy polyethylene glycol (**OCH_3**-PEG_{5k}-**OH**) was evaluated since it is a less expensive homopolymer with similar molecular weight to the block copolymers to be used in targeting experiments. Two reactions were run in parallel. In both, **OCH_3**-PEG_{5k}-**OH** (5 kg mol^{-1}, 0.2 mmol) was dissolved in 19.75 mL DCM with FBA (0.26 mmol) at 0 °C. $TMSCHN_2$ (0.3mmol) was added drop-wise over 4 min and three subsequent additions of 0.15, 0.075, and 0.075 mmol were made in 20 min intervals. After 2 h, the first reaction was ended, while a second reaction mixture was stored, with stirring, in the refrigerator for 24 h. At the end of each reaction period, the solutions were extracted with 20 mL water, dried over anhydrous magnesium sulfate, filtered, concentrated to 3 mL, and precipitated in 300 mL ether. The product was recovered by centrifugation and dried under vacuum.

^{1}H NMR spectra for the two dried products are in Fig S.4, along with the ^{1}H NMR for the starting **OCH_3**-PEG_{5k}-**OH**. For all spectra, the proton peaks corresponding to the methoxy- and hydroxyl- end groups on the PEG were normalized against the ^{13}C shifted proton satellite peak of the CH_2 PEG backbone. The initial **OCH_3**-PEG_{5k}-**OH** spectrum shows a peak of area 0.91 at 3.38 ppm corresponding to the protons of the methyl terminus and a peak of area 0.31 at 2.60 ppm corresponding to the proton of the hydroxyl group. Normalizing the integrated values according to the number of protons in each group, we find that the initial, unreacted mPEG contains 49.5% methyl endgroups, as expected. Similar analysis was used to assess the conversion of the reaction products after 2 h and 24 h. The reaction product contained 76.7% methyl end groups after 2 hours, indicating a conversion of 53.9% of the hydroxyl groups. In contrast, the 24 hour reaction product contained 98.0% methyl endgroups, indicating a conversion of 96.0%. We conclude that the adapted o-methylation procedure should be carried out at 4 °C for 24 h. The discrepancy between the reaction efficiencies suggests that the dilution of reagents requires longer reaction times and higher reagent concentrations to ensure complete conversion.

The 1H NMR peak assignments for the starting **OCH_3**-PEG_{5k}-**OH** and the products are as follows:

- *Monomethoxy-polyethylene glycol* . ^{1}H NMR (500 MHz, $CDCl_3$): δ 3.79 (^{13}C sat., 1H), 3.39 (s, 0.91H), 2.6 (t, 0.31H).
- *Methoxy-polyethylene glycol* . ^{1}H NMR (500 MHz, $CDCl_3$): δ 3.79 (^{13}C sat., 1H), 3.39 (s, 2.07H), 2.6 (t, 0.21H).
- *Methoxy-polyethylene glycol* . ^{1}H NMR (500 MHz, $CDCl_3$): δ 3.79 (^{13}C sat., 1H), 3.39 (s, 3.07H), 2.6 (t, 0.02H).

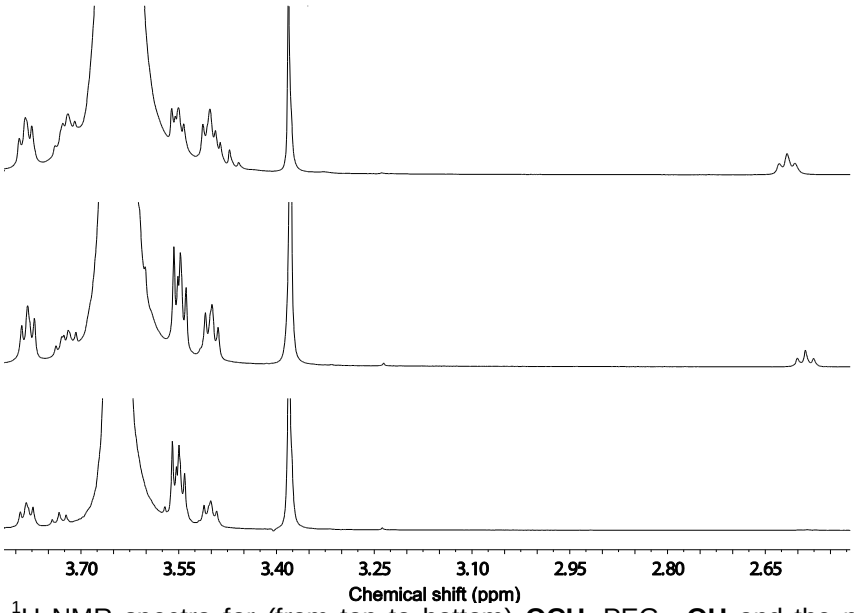

Figure S.4. The ^{1}H NMR spectra for (from top to bottom) **OCH$_3$**-PEG$_{5k}$-**OH** and the product of the o-methylation reaction after 2h and 24h.

To convert the terminal hydroxyl end groups on PS$_m$-*b*-PEG$_n$-**OH** polymers, the reaction protocol described in Chapter 3.1 was followed. Conversion was assessed again by using the the ^{13}C shifted CH_2 protons of the PEG backbone as the reference for integration. The unreacted PS$_{1.5k}$-*b*-PEG$_{5k}$-**OH** showed a broad peak of area 0.85 at 3.38 ppm (Fig. S.5), the expected location of the methyl peak after reaction. This is associated with the specific block copolymer chemistry, is constant, and is used as a baseline value. After subtracting this baseline value from the observed peak in the reaction product, a net increase of 1.69 H was determined. Furthermore, the peak at approximately 2.6 ppm, corresponding to the hydroxyl group, is decreased from 0.49 in the unreacted sample to 0.03 in the reaction product. Using the same analysis method as used with the **OCH$_3$**-PEG$_{5k}$-**OH**, these results indicate a conversion of 95%. The NMR spectra for the PS$_{1.6k}$-*b*-PEG$_{1.8k}$-**OH** and reaction product are also shown in Fig. S.5. The broad baseline peak at 3.38 ppm was still present and was of magnitude 1.92 ppm for this polymer. Accounting for this in the NMR spectra for the reaction product analysis, it is found that a conversion of 97% is achieved for the o-methylation reaction of this polymer.

The ^{1}H NMR peak assignments in Fig. S.5 are as follows.

- *$PS_{1.5k}$-b-PEG_{5k}-**OH***. ^{1}H NMR (500 MHz, $CDCl_3$): δ 3.79 (^{13}C sat., 1H), 3.43-3.3 (br, 1.92H), 2.63 (t, 1.27H).
- *$PS_{1.5k}$-b-PEG_{5k}-**OCH_3** (1.5k-b-5k)* ^{1}H NMR (500 MHz, $CDCl_3$): δ 3.79 (^{13}C sat., 1H), 3.43-3.3 (br, 1.92H), 3.39 (s, 3.2H), 2.63 (t, 0.03H).
- *$PS_{1.6k}$-b-$PEG_{1.8k}$-**OH***. ^{1}H NMR (500 MHz, $CDCl_3$): δ 3.79 (^{13}C sat., 1H), 3.43-3.3 (br, 0.85H), 2.63 (t, 0.49H).
- *$PS_{1.6k}$-b-$PEG_{1.8k}$-**OCH_3***. ^{1}H NMR (500 MHz, $CDCl_3$): δ 3.79 (^{13}C sat., 1H), 3.43-3.3 (br, 0.85H), 3.39 (s, 1.69H), 2.63 (t, 0.03H).

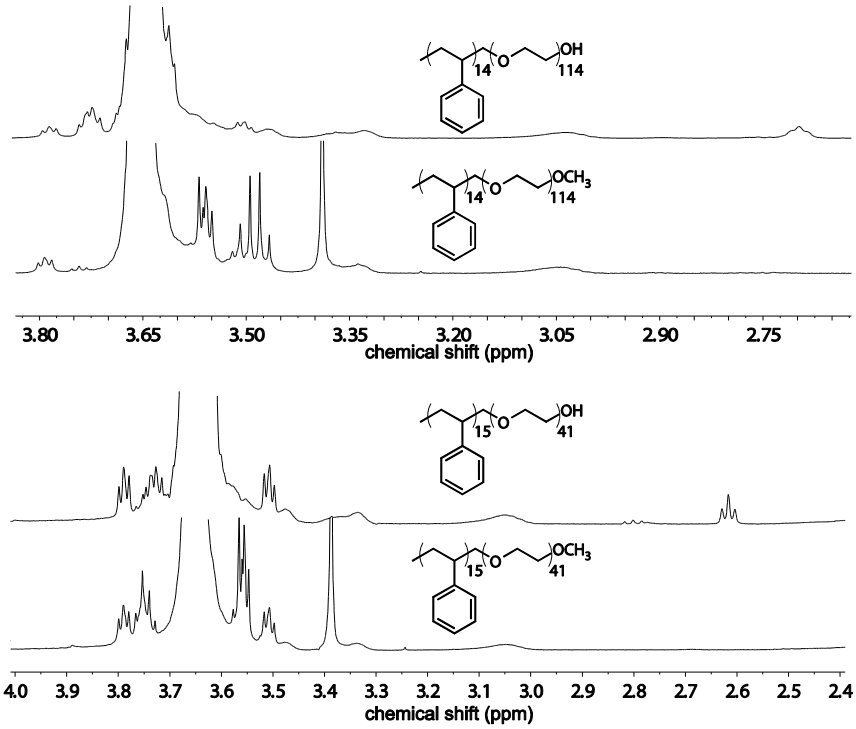

Figure S.5. The 1H NMR spectra for (from top to bottom) $PS_{1.5k}$-*b*-PEG_{5k}-**OH,** $PS_{1.5k}$-*b*-PEG_{5k}-**OCH_3**, $PS_{1.6k}$-*b*-$PEG_{1.8k}$-**OH**, and $PS_{1.6k}$-*b*-$PEG_{1.8k}$-**OCH_3**.

S.4. Nanocarrier assembly by Flash NanoPrecipitation.

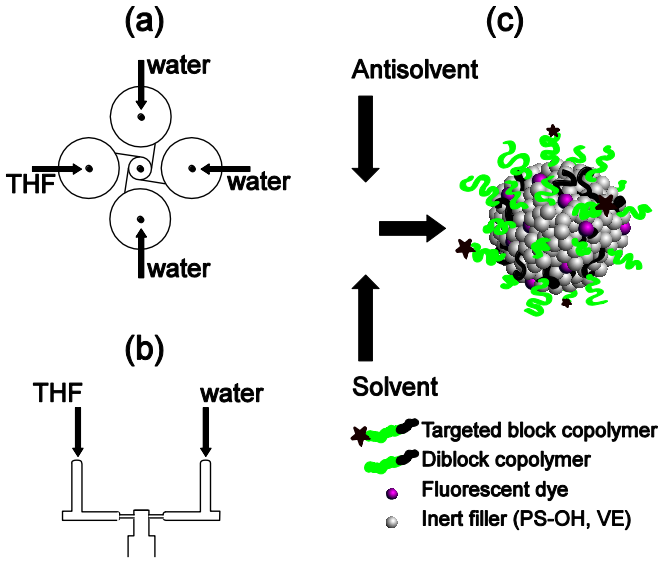

Figure S.6. (a) Schematic of the mixing scheme in a MIVM for NC assembly by Flash NanoPrecipitation (FNP). (b) Mixing geometry for FNP in a CIJ. (c) In both geometries, the THF solution is mixed with water, and nucleation and growth of filler/EtTP5 nuclei is arrested by the adsorption of block copolymers, creating a hydrophobic core-hydrophilic corona structure. Surface functionality is achieved by preparing THF solutions at the desired ratios of block copolymers with and without mannose conjugated to the distal end of PEG.

S.5. Nanocarrier association dependence on time, temperature, and dose.

NCs with average diameters of 115 nm stabilized by $PS_{1.5k}$-*b*-PEG_{5k}-**OH** block copolymers (Formulation 1.1, Fig. 2 inset) were used to determine the time profiles for NC association with J774A.1 and J774E cells at 37°C and 4°C, to evaluate the kinetics of association. Based on prior reports, we investigated the effect of NC properties on binding with J774A.1 [6], while J774E was used in experiments with MR targeted formulations [7]. The results of these experiments are shown in Fig. 2. At 4°C, the NC mass associated with the confluent monolayer in both cell lines reached a steady state at approximately 0.1 µg of NC core mass per cm^2, within the first 20 min for J774A.1 cells, and after 1 h for the J774E clone. At 37°C, where active uptake can occur, a greater extent of NC association in the first 10 min of exposure was observed in J774A.1 cells relative to J774E cells. After 1 h, the NC association increased linearly at the same rate in both cell lines. However, there was a consistently higher level of NC association in the J774A.1 clone. After 3 h of incubation, NC association with the cells at 4°C was 60% lower compared to the same time point in the experiment at 37°C for the J774E clone and 77% lower for the J774A.1 clone.

Formulation 1.1, with hydroxyl-terminated PEG, was also used to determine the cellular association profile with J774E cells as a function of the dose. The doses of the NC core ranged from 30 to 160 µg ml^{-1} and were tested at 37°C and 4°C for 4 h. At 37°C, NC association was linearly related to concentration (R^2=0.98) in the range tested, while at 4°C a plateau in association levels was observed above concentrations of 94 µg ml^{-1} (Fig. 3) [8]. The difference indicates surface attachment without internalization at 4°C, in contrast to continuous cellular internalization at 37°C.

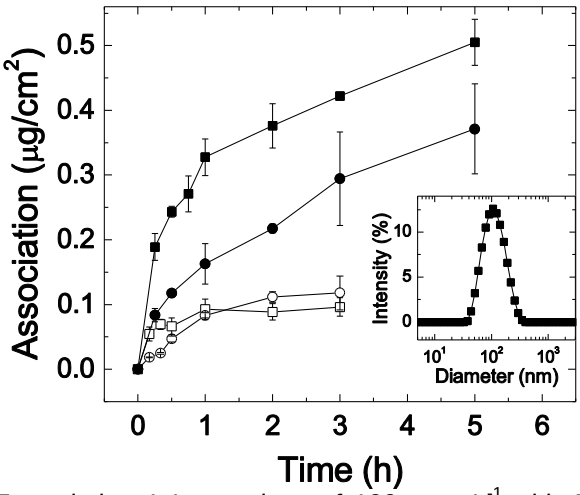

Figure S.7. Association of Formulation 1.1 at a dose of 100 μg mL^{-1} with J774A.1 cells (squares) and J774E cells (circles) at 4°C (open) and 37°C (closed). Inset: particle size distribution for Formulation 1.1, with an intensity average particle diameter of 115 ± 8 nm.

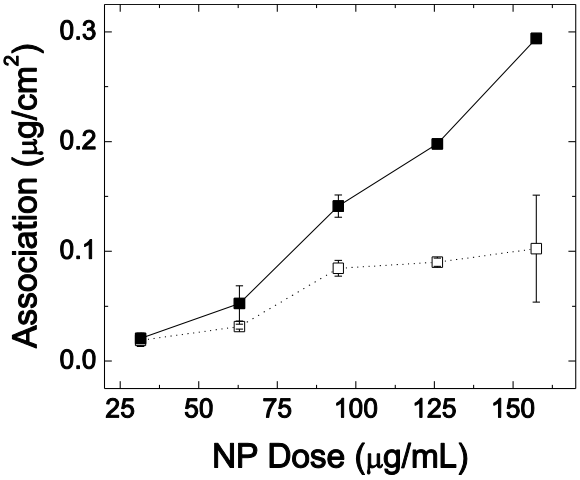

Figure S.8. Extent of association of $PS_{1.5k}$-OH NCs stabilized by $PS_{1.5k}$-*b*-PEG_{5k}-**OH** (Formulation 1.1) at 4°C (□) and 37°C (■) at indicated doses.

S.6. Association vs. size for mannose receptor targeted formulations.

Due to variation contributed by the human element during mixing to produce mannose receptor targeted formulations in Table 2, there were differences in the measured intensity average diameter. The uptake data is plotted versus the intensity average diameter to determine if the size of the NCs contributed to the observed trends in the data. In this linear regression, the null hypothesis is $b = 0$ and the alternate hypothesis is $b \neq 0$, where b is the slope of the line fit to the data. The slope of the line is -1.46×10^{-4}, with a standard error of 6.73×10^{-4}. The value of the p statistic in this regression is 0.832. Therefore, the null hypothesis cannot be rejected, and there is no statistically significant relationship between nanocarrier core uptake and particle diameter.

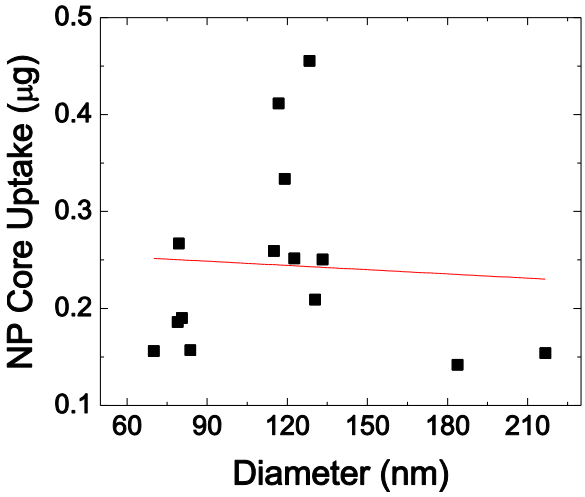

Figure S.9. The experimentally measured nanocarrier association is plotted against the intensity average diameter of the nanocarrier formulations as measured by DLS. Linear regression reveals that there is no statistically significant influence of particle size on nanocarrier association.

S.7. References

[1] W. Hayes, H.M.I. Osborn, S.D. Osborne, R.A. Rastall, B. Romagnoli, One-pot synthesis of multivalent arrays of mannose mono- and disaccharides, Tetrahedron, 59 (2003) 7983-7996.

[2] M. Dowlut, D.G. Hall, O. Hindsgaul, Investigation of nonspecific effects of different dyes in the screening of labeled carbohydrates against immobilized proteins, Journal of Organic Chemistry, 70 (2005) 9809-9813.

[3] S.Y. Zhang, D.H. Adamson, R.K. Prud'homme, A.J. Link, Photocrosslinking the polystyrene core of block-copolymer nanoparticles, Polymer Chemistry, 2 (2011) 665-671.

[4] T.R. Chan, R. Hilgraf, K.B. Sharpless, V.V. Fokin, Polytriazoles as copper(I)-stabilizing ligands in catalysis, Organic Letters, 6 (2004) 2853-2855.

[5] T. Aoyama, T. Shioiri, New Methods and Reagents in Organic-Synthesis .91. Trimethylsilyldiazomethane - a Convenient Reagent for the O-Methylation of Alcohols, Tetrahedron Letters, 31 (1990) 5507-5508.

[6] A. Rehor, H. Schmoekel, N. Tirelli, J.A. Hubbell, Functionalization of polysulfide nanoparticles and their performance as circulating carriers, Biomaterials, 29 (2008) 1958-1966.

[7] Z.R. Cui, C.H. Hsu, R.J. Mumper, Physical characterization and macrophage cell uptake of mannan-coated nanoparticles, Drug Development and Industrial Pharmacy, 29 (2003) 689-700.

[8] S. Martin, R.G. Parton, Lipid droplets: a unified view of a dynamic organelle, Nat. Rev. Mol. Cell Bio., 7 (2006) 373-378.